# 自黏附硅橡胶表面水凝胶润滑层的原位生长及其性能研究

冯海燕，李谋吉，于强亮，杨武芳，周春宇，马延飞，麻拴红，于波，周峰

## In-Situ Growth of Hydrogel Lubrication Film on Self-Adhesive Silicon Elastomer Surface and Its Performance

FENG Haiyan, LI Mouji, YU Qiangliang, YANG Wufang, ZHOU Chunyu, MA Yanfei, MA Shuanhong, YU Bo, ZHOU Feng

您可能感兴趣的其他文章

Articles you may be interested in

关注微信公众号，获得更多资讯信息

# 自黏附硅橡胶表面水凝胶润滑层的原位生长及其性能研究

冯海燕[1,2], 李谋吉[1,2], 于强亮[1], 杨武芳[1], 周春宇[1,3], 马延飞[1], 麻拴红[1], 于　波[1*], 周　峰[1*]

(1. 中国科学院兰州化学物理研究所 固体润滑国家重点实验室, 甘肃 兰州 730000;

2. 中国科学院大学, 北京 100049;

3. 烟台中科先进材料与绿色化工产业技术研究院, 山东 烟台 264010)

**摘　要:** 在水体环境中, 水凝胶润滑薄膜与基底之间可逆以及便捷的结合是润滑材料领域的挑战之一. 本研究中将自黏附硅橡胶与具有润滑功能的水凝胶相结合, 获得了一种具有可逆湿黏附功能的水凝胶润滑材料. 在低交联度聚二甲基硅氧烷(PDMS)表面/亚表面填埋引发剂二苯甲酮, 通过表面光引发聚合的方式使其表面生长具有润滑功能的水凝胶-聚(丙烯酸-co-丙烯酰胺)[P(AA-co-AAm)]. 研究结果表明: 水凝胶与硅橡胶基材在交界处形成连接致密的一体结构. 当丙烯酸与丙烯酰胺摩尔比为1:1时, 水凝胶表现出优异的摩擦学性能, 并且力学强度较高. PDMS的模量随着固化剂含量增加而升高, 而摩擦系数则呈现相反的趋势; 当PDMS硅烷预聚体与固化剂质量比例为30:1时具有较好的机械性能、黏附性能以及较低的摩擦系数. 所制备的可黏附水凝胶使得水润滑材料具有水下可黏附特性, 该体系与金属、陶瓷以及聚合物等多种基底表面均具有良好的黏附性能, 多次重复黏附测试后, 黏附强度基本保持不变. 该方法解决了水凝胶润滑材料与基底的结合问题, 有望为医疗器械表面的润滑改性提供一种新思路.

**关键词:** 水凝胶; 润滑; 原位生长; 黏附; 表面改性

**中图分类号:** TH117.2　　　　　　　　**文献标志码:** A　　　　　　　　**文章编号:** 1004-0595(2023)04–0347–11

# In-Situ Growth of Hydrogel Lubrication Film on Self-Adhesive Silicon Elastomer Surface and Its Performance

FENG Haiyan[1,2], LI Mouji[1,2], YU Qiangliang[1], YANG Wufang[1], ZHOU Chunyu[1,3],
MA Yanfei[1], MA Shuanhong[1], YU Bo[1*], ZHOU Feng[1*]

(*1. State Key Laboratory of Solid Lubrication, Lanzhou Institute of Chemical Physics,
Chinese Academy of Sciences, Gansu Lanzhou 730000, China*

*2. University of Chinese Academy of Sciences, Beijing 100049, China*

*3. Yantai Zhongke Research Institute of Advanced Materials and Green Chemical
Engineering, Shandong Yantai 264010, China*)

**Abstract**: Reversible and convenient bonding underwater between hydrogel lubrication film and substrate is one of the challenges in the field of tribology. In this study, the lubrication film was combined with the silicone rubber to prepare hydrogel-lubricated silicone rubber with reversible wet adhesion. Polydimethylsiloxane (PDMS) with low degree of crosslink was used as an underwater adhesion material, and the initiator benzophenone was buried on its

surface/subsurface, then the hydrogel lubricating film Poly (acrylic acid-co-acrylamide) [P(AA-co-AAm)] was grown on the surface through surface photopolymerization. The interface structure of obtained hydrogel-lubricated silicone rubber was explored by field emission scanning electron microscope (FESEM). The effects of ratio of hydrogel monomers, concentration of crosslinking agent, and polymerization time on performance of films were explored. The ratio of curing agent in PDMS was adjusted to explore its effects on adhesion and tribological properties of films. The results showed that a densely connected structure formed between the interface of hydrogel and PDMS. As the content of acrylic acid increased, the friction coefficient showed a trend of first decrease and then increase. When the content of acrylamide was further reduced, the acrylic acid segment absorbed water easily and swelled, leading to the reduction of mechanical strength and increase of friction coefficient. When the molar ratio of acrylic acid to acrylamide was 1:1, the hydrogel exhibited excellent tribological properties and mechanical strength. When the content of the crosslinking agent increased, the mechanical properties of hydrogel was optimized, and it exhibited better lubrication property. In addition, the modulus of PDMS increased as the content of curing agent, while the friction coefficient showed the opposite trend.; when the mass ratio of PDMS silane prepolymer to curing agent was 30:1, PDMS had favorable mechanical properties, adhesion performance and low friction coefficient. The prepared hydrogel-lubricated silicone rubber made the hydrogel adhesive underwater and endowed the silicone rubber with excellent lubrication and anti-wear properties. PDMS substrate was worn severely in the sliding direction after the friction test, its surface was damaged and there were obvious pits. In contrast, the hydrogel film only produced very slight scratches. The wear scar of the hydrogel was investigated, and the results showed that after nearly 3 000 cycles, the surface layer of the hydrogel film did not change much, which proved that the hydrogel film had excellent resistance to abrasiveness compared to PDMS. After repeated adhesion tests, the hydrogel film still had excellent adhesion properties. In addition, the hydrogel-lubricated silicone rubber had different adhesion on two sides. PDMS side showed good adhesion to titanium alloy, PTFE, and ceramics underwater while the hydrophilic hydrogel layer had no adhesion to titanium alloys, ceramics, etc. underwater, and directly falls off the surface of the materials.

**Key words**: hydrogel; lubrication; in-situ growth; adhesive; surface modification

水凝胶因具有高含水率、弹性力学性能、高生物相容性以及类组织特性,在组织工程[1]、软体机器人[2-4]、药物递送[5]和植入式电子[6-7]等领域有着广泛的应用. 自上世纪90年代以来,国内外科学家开展了大量水凝胶摩擦相关的研究工作[8-10]. Qu等[11]采用碱诱导网络解离策略,制备顶层和底层性能不同的层状水凝胶材料,该方法也可用于研制层状水凝胶润滑导管,其内表面和外表面均具有润滑特性. Piers 等[12]将仿生边界润滑剂聚(2-甲基丙烯酰氧基乙基磷酰胆碱) (PMPC)聚合物网络掺入双相凝胶中,得到具有边界和双相润滑能力的水凝胶. Wang等[13]通过集成响应性超分子系统,研究制备了一种具有可逆光响应性超分子润滑能力的半转换水凝胶,可以实现智能摩擦调控. 然而,目前的研究仅仅集中于本体水凝胶,而水凝胶与基底之间很难形成有效的黏附[14-16],这极大地影响了改性表面润滑性能的稳定性和耐久性[17-18]. 因此,可黏附性对于水凝胶在各个方面的应用至关重要,尤其是在医疗器械表面的润滑改性方面,亟需解决润滑层与基底的结合问题.

在过去的十年中,水凝胶与基底之间锚固方面的研究已经取得重大进展,Zhao等[19]基于可溶胀聚合物(硅橡胶、聚氨酯、聚氯乙烯和丁腈橡胶等)表面和亚表面填埋引发剂,原位引发水凝胶的聚合,基于网络互穿实现凝胶与聚合物基底之间的高度结合,有效降低了材料表面的摩擦系数. Xu等[20]利用黏性引发层(SIL) [SIL@ UV-SCIRP]的紫外触发表面催化引发自由基聚合(UV-SCIRP),生长水凝胶涂层,可实现各种医疗器械外表面的水凝胶涂层改性. 此外,Cui等[21]通过将带负电荷的含羧基水凝胶与阳离子寡糖通过单向浸渍的方法梯度静电络合,形成一种新型的水凝胶湿胶黏剂,其两面对组织具有明显的黏附性差异,一面具有强黏附性能,而另外一面具有抗黏附性能. 近期,本研究团队利用二价铜离子与邻苯二酚的配位作用,采用水下胶黏剂聚(多巴胺甲基丙烯酰胺-甲氧基乙基丙烯酸酯)修饰聚乙烯醇/甘油-单宁酸/$Cu^{2+}$水凝胶表面制备了一种水下可黏附的自清洁水凝胶. 其优势在于水凝胶可根据应用场景黏附到各种表面,并可随时进行更换,多次反复使用[22]. 然而,复杂的修饰方法、不可逆的黏附以及不稳定的水下黏附性能限制了其在很多领域的应用.

原位生长制备复合材料能够结合不同材料的优点,在制备复合材料领域有着广泛的应用[23-24]. Wang等[24]

以多孔材料为灵感, 通过在聚氨酯(PU)海绵上原位生长新型胶粘剂/黑色水凝胶, 制备了多孔水凝胶海绵, 实现了太阳能驱动的持久高效水分蒸发. Jin等[25]在有机水凝胶聚电解质上一步原位生长聚苯胺, 制备了同时具有防冻高拉伸超级电容器(AF-SSC). 本研究中采用在水下具有可逆黏附特性的低交联度的聚二甲基硅氧烷(PDMS)作为黏附材料[26], 通过在其表面和亚表面填埋光引发剂, 基于表面光引发聚合原位生长的方法实现可黏附水凝胶润滑材料的制备. 其中, 水凝胶层与PDMS胶具有较强的结合. 所制备的材料能够黏附于各类无机以及有机材料实现表面润滑改性, 并且能够实现多次可逆黏附. 凝胶层赋予了各类基材优异的减摩抗磨性能. 这种制备方法有望为医疗器械的表面润滑改性提供一种新思路.

# 1　试验部分

## 1.1　试验材料及制备

### 1.1.1　试验材料

丙烯酸(Acrylic acid, AAc), 质量分数为99%, 购自Sigma-Aldrich公司; 丙烯酰胺(Acrylamide, AAm)质量分数为99%, 购自J&K Chemical 公司; N, N-亚甲基双丙烯酰胺(Methylene-bisacrylamide, MBA), 质量分数为99%, 购自Sigma-Aldrich公司; α-酮戊二酸, 质量分数为98%, 购自Sigma-Aldrich公司; 二苯甲酮, 质量分数为99%, 购自上海麦克林生化科技有限公司; 硅烷预聚体, 固化剂 (SYLGARD184, Dow Corning); 无水乙醇, 化学纯度, 购自天津化学试剂有限公司产品; 所有试验用水均为去离子水.

### 1.1.2　P(AAc-co-AAm)水凝胶制备

首先配置不同摩尔比例(5:1、3:1、1:1、1:3以及1:5)的AAm与AAc作为水凝胶预聚液. 然后加入摩尔数为单体总摩尔量0.3%的交联剂MBA, 以及摩尔数为单体总摩尔量0.03%的光引发剂α-酮戊二酸, 搅拌均匀待用.

将通过上述方法配置的不同比例水凝胶预聚液倒于9 cm×9 cm×0.35 mm聚苯乙烯模板间, 紫外光(功率: 36 W, 照射距离: 5 cm)照射下引发聚合1 h. 将摩尔数分别为单体总摩尔量0.1%、0.5%、0.7%和0.9%的交联剂加入AAc与AAm摩尔比例为1:1的水凝胶预聚液中, 紫外光照射下聚合1 h得到水凝胶.

### 1.1.3　PDMS基底的制备

将硅烷预聚体与固化剂分别以不同质量比(10:1、20:1、30:1、40:1和50:1)进行混合, 然后加入混合液1/3体积的正己烷, 搅拌均匀除去气泡. 最后将混合液

铺展于培养皿, 置于烘箱, 加热至50 ℃固化3 h.

### 1.1.4　硅橡胶表面水凝胶层的制备

依次采用去离子水、乙醇超声清洗PDMS表面, 并采用氮气将表面吹干, 然后其中一面在100 W功率下氧气等离子体处理1 min (FEMTO plasma cleaner), 再采用无水乙醇洗净、干燥. PDMS一面密封, 另一面置于含有10%质量分数的二苯甲酮的无水乙醇溶液中浸泡20 min, 再用无水乙醇冲洗表面, 干燥后备用. 将AAc与AAm摩尔比例为1:1的水凝胶预聚液铺展于PDMS表面, 上面盖玻璃板隔绝空气, 放置于紫外灯下分别聚合1、2、3和4 h.

## 1.2　试验方法

### 1.2.1　表征

采用全反射傅里叶变换红外光谱(ATR-FTIR, Nicolet iS10, Thermo scientific, USA)测定水凝胶的化学结构, 分辨率为4 cm$^{-1}$. 利用Thermo ESCALAB 250Xi X射线光电子能谱仪(Thermo maple plain, XPS)进行成分分析. 采用场发射扫描电子显微镜(FESEM, JSM-6701F, JEOL Inc, Japan)观察样品的表面及截面形貌, 并在20 kV加速电压下用电子色散谱(EDS)进行截面成分分析.

### 1.2.2　黏附性能测试

通过万能材料试验机(EZ-Test, SHIMADZU)进行黏附试验. 将1 cm×1 cm的玻璃块轻轻压在水凝胶上并达到预设力(0.1、0.5、1.0、1.5和2.0 N), 然后以恒定速率100 mm/min抬离, 得到黏附曲线, 上述测试均重复5次. 预加载力由程序控制, 并可保证试验中预设力的准确性和一致性. 最大正值表示最大预紧强度, 而黏附强度是通过测量的拉脱力除以接触面积(1 cm$^2$)得到, 黏附强度为负值.

### 1.2.3　力学强度测试

采用万能材料试验机进行力学试验. 拉伸速率保持在100 mm/min. 弹性模量由应力-应变曲线中应变比在5%~15%范围内的斜率计算. 拉伸应力计算方法为拉力除以样品横截面面积. 压缩性能使用万能材料试验机进行评估, 将水凝胶样品浇筑成圆柱形, 压缩的速度控制在50 mm/min, 压缩应变为60%, 上述测试均重复5次.

### 1.2.4　摩擦学性能测试

通过摩擦试验机(CSM Co Ltd, Switzerland)考察水凝胶材料的摩擦学性能. 将水凝胶块固定于下托盘, 选取直径(Φ)为6 mm的PDMS球作为摩擦对偶, 摩擦介质为水, 采用往复模式, 在不同频率及载荷下进

行摩擦学性能考察. 摩擦学性能测试之前, 所有样品都在相应溶剂中浸泡并达到溶胀平衡.

## 2 结果与讨论

### 2.1 可黏附水凝胶润滑材料的制备及表征

低交联度的PDMS对各种类型的基底具有较好的干湿黏附特性, 在其表面修饰水凝胶, 可制备与基底黏附的水凝胶润滑硅橡胶[26-27]. 调整硅烷预聚体与固化剂的比例得到机械和黏着性能优异的PDMS基底. 利用溶胀驱动将引发剂二苯甲酮引入PDMS表层, 然后含亲水性引发剂α-酮戊二酸的水凝胶预聚液在PDMS表层通过原位光引发聚合的方式生长水凝胶润滑层(图1)[28]. 吸附在PDMS表层的二苯甲酮可作为水凝胶聚合物与PDMS基底聚合物链交联的接枝剂和氧清除剂, 此外, 二苯甲酮在水中的不溶解性阻止了其从PDMS表层向水凝胶预聚液中的扩散[19].
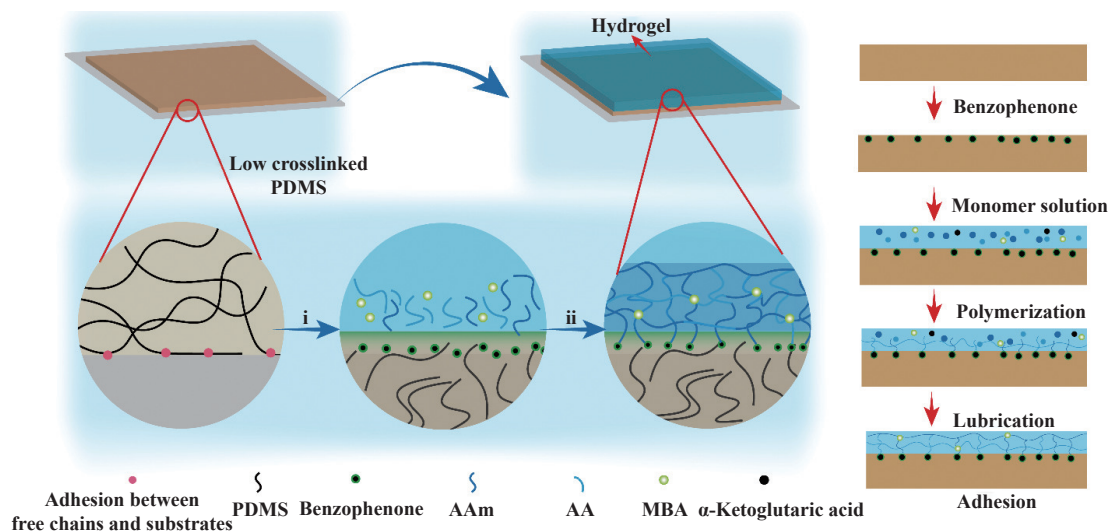


Fig. 1    Schematic illustration of hydrogel-lubricated silicone rubber preparation procedures

图 1    可黏附水凝胶润滑硅橡胶的原位生长示意图

图2所示为所制备润滑硅橡胶的红外光谱与XPS谱图, 由图2(a)红外光谱可知, 仅在PDMS可黏附面观察到Si-O-Si键的伸缩振动峰(1 013 cm$^{-1}$), 而在水凝胶面可以观察到3 340 cm$^{-1}$处的N-H伸缩振动峰, 1 650 cm$^{-1}$处的C(=O)-NH$_2$中C=O的伸缩振动峰以及1 312 cm$^{-1}$处的-C(C=O)-O中C-O的吸收峰. 由图2(b~d) XPS表征结果可知, PDMS可黏附面Si 2p信号较强, 并且水凝胶表面观察到N 1s信号峰, 而在PDMS面并未观察到. 以上结果表明成功制备了PDMS表面水凝胶.

水凝胶与PDMS基底之间的结合尤为重要, 因此采用SEM获取了硅橡胶表面修饰水凝胶层后的截面形貌照片, 结果如图3所示. 由图3(a)可知, 整个体系没有断层, 结合紧密, 上层为具有多孔结构的水凝胶, 水凝胶的表面形貌[图3(b)]与其具有同样的结构. 此外, 从截面SEM照片可以看出在靠近PDMS部分水凝胶的多孔结构消失, 形成致密的结构[图3(c)], 原因可能是PDMS端吸附的引发剂使得靠近PDMS端水凝胶部分引发剂总体含量增多, 聚合物链密度增大, 与水凝胶在交界处形成连接致密的一体结构, 而下层为致密的PDMS. 利用EDS对水凝胶与PDMS界面进行成分分析, 结果如图3(d~f)所示, Si元素只富集于PDMS端, 并存在明显的界限, 为PDMS中含有的特征元素; 同样地, N元素不仅富集于水凝胶端, 而且在交界处依然存在, 但分布骤减, 为水凝胶中含有的特征元素; O元素贯穿于整个切面, 在PDMS和水凝胶中均存在. 尽管元素分布具有明显的界限, 然而水凝胶和PDMS基底表现为1个整体, 结合紧密. 在水中浸泡不同时间后对可黏附润滑硅橡胶的断面进行观察, 结果如图4所示, 由图可知, 浸泡9天后, 水凝胶层发生轻微溶胀, 界面处没有发生任何变化. 以上结果表明水凝胶利用油溶性引发剂在PDMS表面成功聚合.

### 2.2 水凝胶的性能优化

水凝胶的化学组成影响其力学性能及摩擦学性能. 通过调整AAc和AAm的摩尔比例, 聚合得到不同化学组成的水凝胶, 对其力学性能和摩擦学性能进行探究, 结果如图5所示. 由图5(a)可知, 随着AAc与AAm单体摩尔比例减小, 水凝胶的拉伸强度先增大后减小. 当AAc与AAm的单体摩尔比例为3:1时, 水凝胶的拉
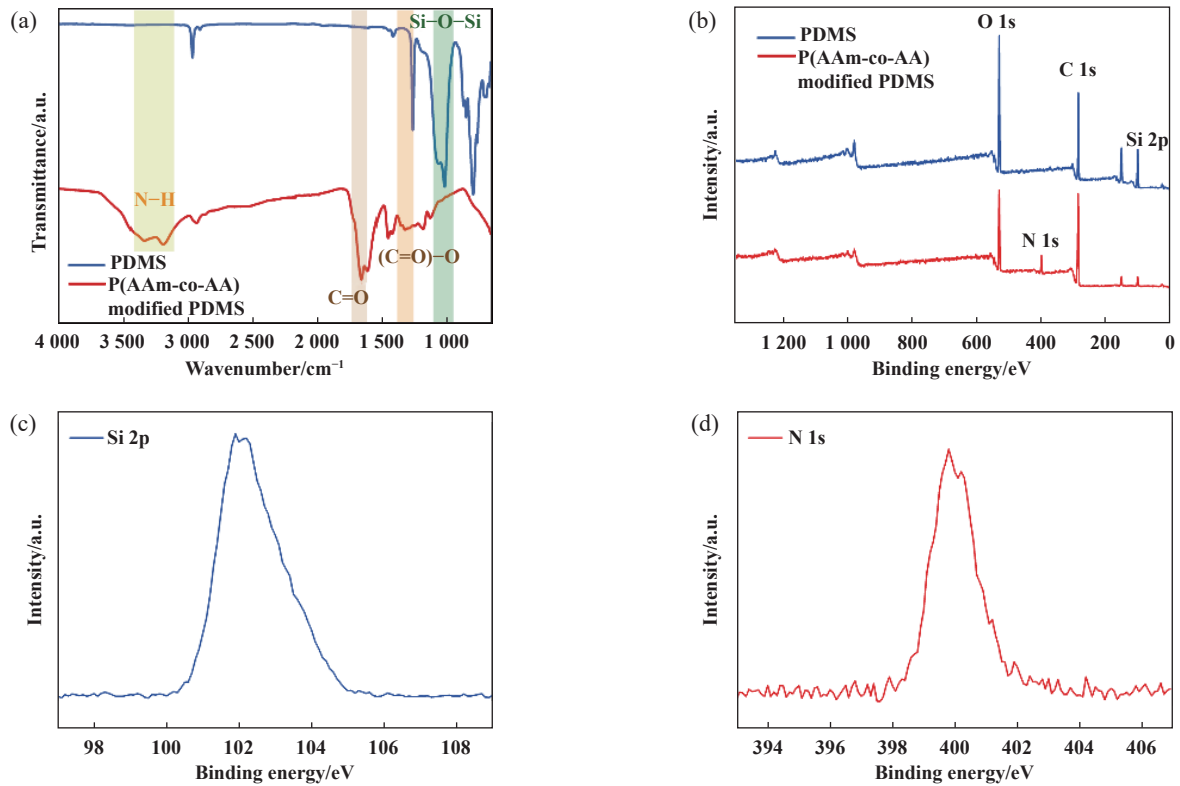
Fig. 2　Characterization of the surface of lubricated silicone rubber: (a) FT-IR; (b) XPS; (c) Si 2p
spectrum of PDMS material; (d) N 1s spectrum of hydrogel material

图 2　润滑硅橡胶表面的表征：(a)红外光谱；(b) XPS图谱；(c) PDMS材料的Si 2p图谱；(d)水凝胶材料的N 1s图谱
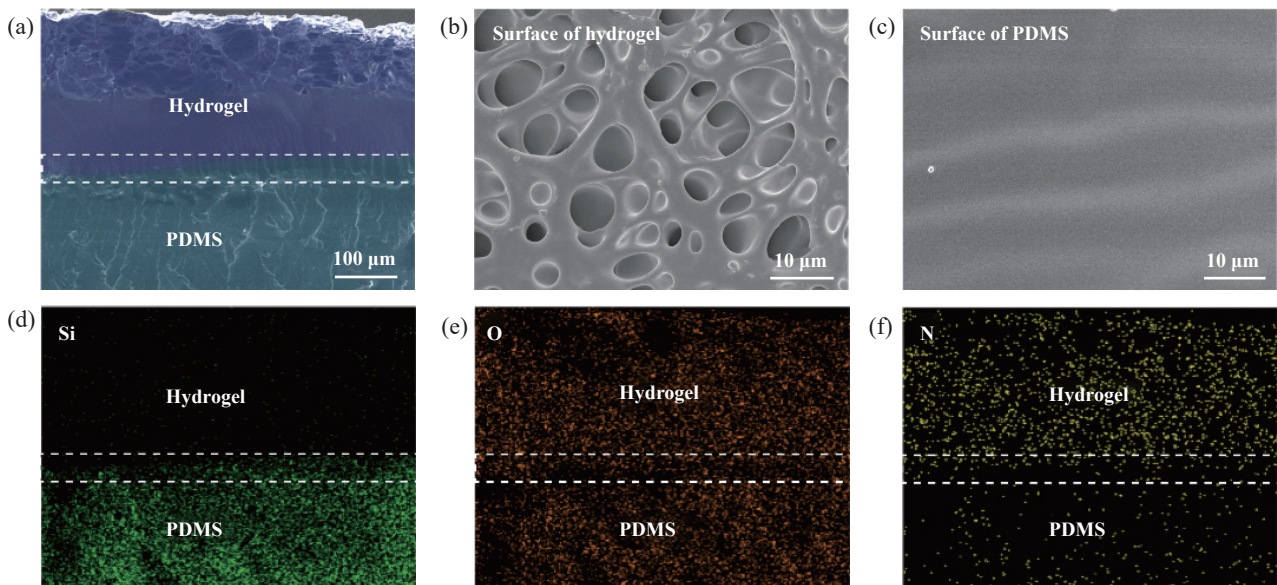


Fig. 3　SEM micrographs of hydrogel lubricated silicone rubber morphology: (a) section structure; (b) hydrogel
surface; (c) PDMS; EDS analysis of cross-section structure: (d) Si; (e) O; (f) N

图 3　水凝胶润滑硅橡胶形貌的SEM照片：(a)断面结构；(b)水凝胶表面；(c) PDMS表面；
断面结构的EDS分析：(d) Si；(e) O；(f) N

伸强度可达到0.31 MPa，而当单体摩尔比例下降至
1:5时，拉伸强度下降至0.06 MPa. 与拉伸强度趋势相
似，水凝胶的压缩强度随着丙烯酸比例的增大不断升

高，并且压缩模量由0.058 MPa增强至0.1 MPa，当丙
烯酸与丙烯酰胺的单体摩尔比例为1:1、3:1和5:1时，
压缩模量变化较小[图5(b)]. AAc聚合得到刚性链段，

使得水凝胶的强度增加；AAm聚合得到相对柔性的链段，使得水凝胶韧性增加[29-30]. P(AAc-co-AAm)水凝胶的交联密度与AAc的加入量成正比[29]，随着AAc比例的增大，水凝胶的强度增大[图5(d)]. 丙烯酸与丙烯酰胺之间易形成氢键，当丙烯酸单体过多，形成氢键数量减少，强度有所降低[31]. 单体比例对摩擦系数的影响如图5(d)所示，随着丙烯酸含量的增大，摩擦系数呈

现先减小后增大的趋势. 丙烯酰胺是非离子型单体，相对于丙烯酰胺，丙烯酸与水分子之间作用力更强，即水化作用更强[32-33]. 形成的水化层对剪切产生类似流体的响应，并降低接触下的黏结力，从而在两个界面相互滑动时充分避免了直接的粗糙接触[12, 34-35]，从而降低摩擦力；当丙烯酰胺含量进一步降低时，过量的丙烯酸链段在摩擦条件下极易吸水溶胀[35-36]，力学



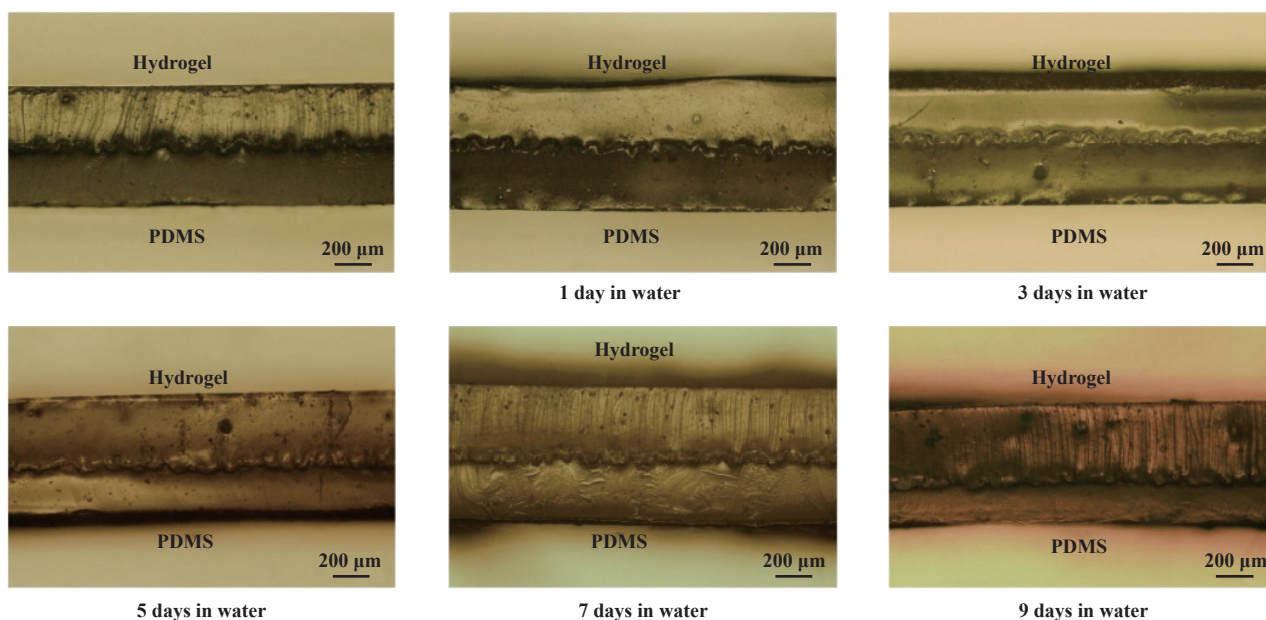Fig. 4    SEM micrographs of section diagram of hydrogel-lubricated silicone rubber soaked in water for different times

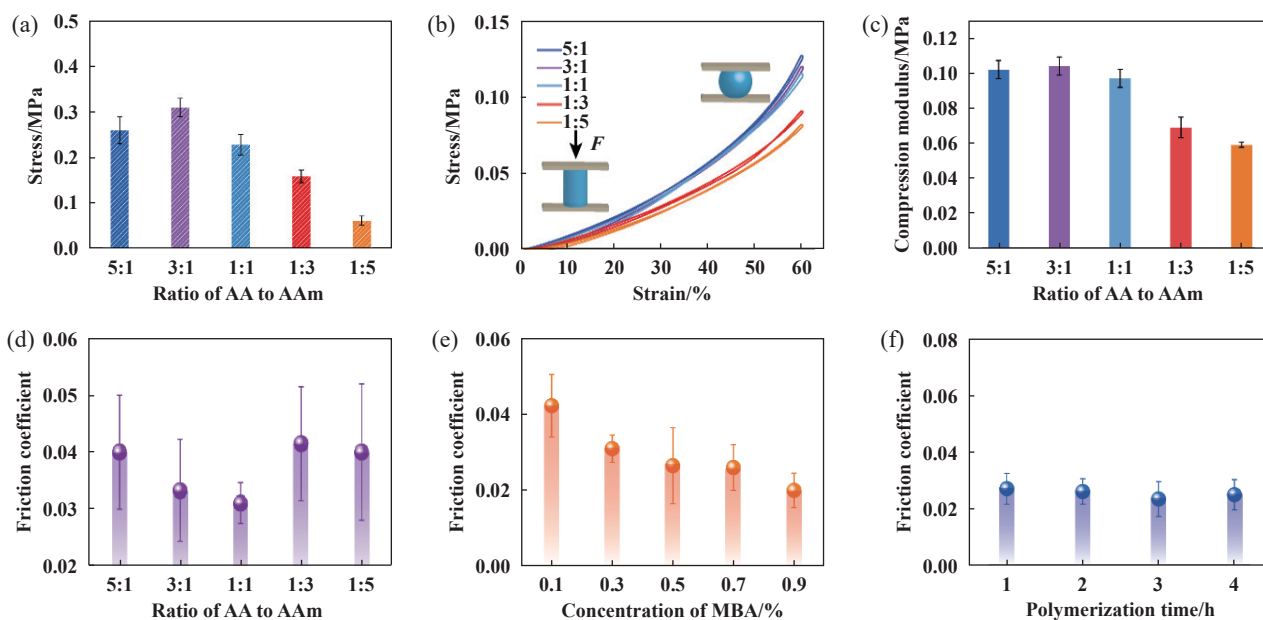图 4    水中浸泡不同时间后可黏附润滑硅橡胶的断面的SEM照片



Fig. 5    Effect of monomer molar ratio on hydrogel properties: (a) tensile properties; (b) compressive strength; (c) compression modulus. the effect factors of friction coefficient: (d) monomer ratio; (e) crosslinking agent concentration; (f) polymerization time

图 5    单体摩尔比例对水凝胶性能的影响：(a)拉伸性能；(b)压缩强度；(c)压缩模量，摩擦系数的影响因素：(d)单体比例；(e)交联剂浓度；(f)聚合时间

强度有所降低, 摩擦系数增大. 因此, 水凝胶单体比例选择1:1. 由图5(e)可知, 随着交联剂含量的增大, 摩擦系数减小, 因为交联剂含量的增大, 使得水凝胶共价网络增多, 并且网络之间交联点增多, 在一定程度上机械性能得到优化, 在进行承载摩擦时表现出较好的润滑效果. 由图5(f)可知, 水凝胶聚合时间对于摩擦系数影响较小, 原因为紫外光下自由基引发聚合速率较快. 因此, 水凝胶中最优的单体比例为1:1, 引发剂含量为单体总摩尔量的0.9%, 紫外光下聚合时间为1 h.

## 2.3 硅橡胶基底性能优化

　　PDMS基底制备过程中硅烷预聚体和固化剂的质量比会对其力学性能和黏附性能产生影响. 如图6(a)所示, 随着固化剂比例的减小, PDMS基底的拉伸强度呈现下降趋势. 其拉伸强度从6.7 MPa (硅烷预聚体和固化剂比例为10:1)降低至0.1 MPa (50:1). 其对应的弹性模量从1.6 MPa降低至0.1 MPa [图6(b)]. 相反地, PDMS的黏附强度随着固化剂比例的降低而不断升高, 当固化剂摩尔比例降低至30:1或更低时, 其黏附强度保持在同一水平[图6(c)], 这是因为固化剂的减少会使得PDMS中自由链数量增多, 增强了与基底的相

互作用[28]. 此外, 还考察了预加载力对PDMS (30:1)在空气和水下两种环境中的黏附强度的影响[图6(d)]. 施加0.1 N的预加载力, 其黏附强度在5.7 kPa左右, 并且随着预加载力的增加, 其黏附强度不断增大, 当超过1 N时趋于平缓(黏附强度在18~20 kPa). 预加载力的增加使得PDMS与测试基底的接触面积增大, 而当预加载力达到一定值后, 力的增加不会引起接触面积产生较大的变化, 因而其黏附强度呈现出先增大后趋于平缓的趋势. 水下的黏附强度随预加载力的增加变化较小, 由1.2 kPa增加至1.5 kPa.

　　进一步探究了PDMS中固化剂比例对上层水凝胶润滑层摩擦学行为的影响(图7). 当法向载荷为0.2 N, 滑动频率为1 Hz时, 可黏附润滑硅橡胶的摩擦系数随着PDMS中硅烷预聚体与固化剂比例的增加而增大. 当硅烷预聚体与固化剂比例为10:1时, PDMS弹性模量为1.6 MPa, 其对应的水凝胶层的摩擦系数为0.017; 当比例增加至50:1时, PDMS弹性模量为0.1 MPa, 水凝胶的摩擦系数增加至0.045. 在施加载荷的过程中, PDMS基底模量小时摩擦过程中会产生更大的弹性形变[37]. 本体系中摩擦力来源于切向阻力和机械变形,
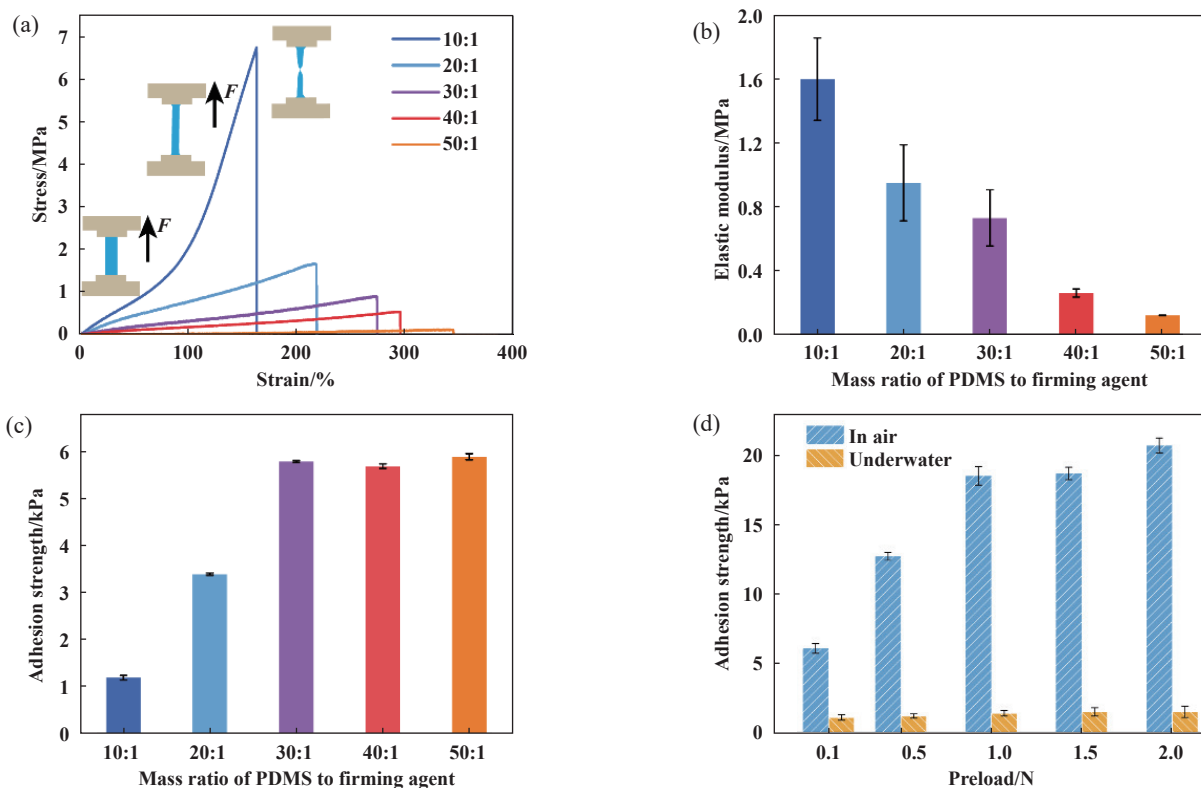


Fig. 6　The effect of curing agent ratio on PDMS properties: (a) mechanical properties; (b) elastic modulus; (c) adhesion strength,
(d) the effect of preloading force on adhesion strength under different conditions

图 6　固化剂比例对于PDMS性能的影响: (a)力学性能; (b)弹性模量; (c)黏附强度,
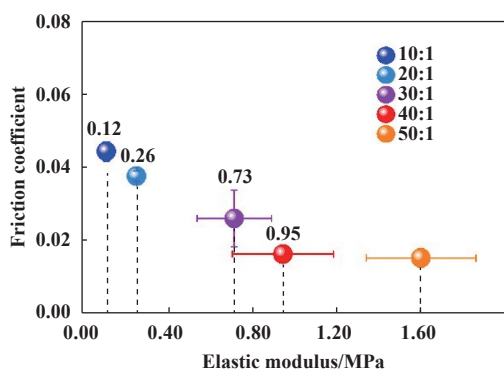(d)预加载力在不同条件下对黏附强度的影响

Fig. 7 The effect of elastic modulus of PDMS on the friction coefficient

图 7 PDMS弹性模量对于摩擦系数的影响

基底模量增加使得界面弹性变形减小,切向变形的阻力减小,摩擦力减小[38]. 综上可知,当硅烷预聚体与固化剂比例为30:1时,PDMS具有较好的机械性能(0.9 MPa)和优异的黏附强度.

## 2.4 可黏附水凝胶润滑硅材料的摩擦性能探究

以PDMS半球作为摩擦副,测试PDMS表面修饰水凝胶层的摩擦学性能(图8). 结果表明水凝胶润滑硅橡胶的摩擦系数随着载荷的增大呈现正相关变化趋势. 这种现象可归因于当载荷增大时,法向位移变大,摩擦副滑动时受到法向阻力也增大,表现为摩擦系数增大[39]. 当施加荷载为0.2 N时,随着滑动频率的增加,

润滑硅橡胶的摩擦系数呈现先减小后增大的趋势,但总体变化区间较小,最低的摩擦系数为0.029,最高的摩擦系数为0.035. 这些结果表明频率的变化对润滑硅橡胶的摩擦系数没有显著影响. 在载荷为0.2 N和频率为1 Hz的条件下进行摩擦测试,经历2 500个循环后,其摩擦系数仍低于0.04,并且摩擦系数没有突增. 相反地,PDMS基底具有较大地摩擦系数,并且不断磨损(图9). 以上试验结果说明所制备的润滑硅橡胶相较于纯硅橡胶具有良好的耐磨性.

摩擦测试后PDMS基底和水凝胶的磨痕形貌的SEM照片如图9所示,相较于摩擦前[图9(a1)],摩擦试验后PDMS基底在滑动方向磨损严重,表面被破坏,有明显的凹坑[图9(b1)];而水凝胶层仅产生轻微的划痕[图9(b2)]. 在经历近3 000个循环后,水凝胶表层未发生明显的变化,证明水凝胶润滑层的存在使得硅橡胶具有优异的耐磨性.

## 2.5 可黏附水凝胶润滑材料的黏附行为研究

可黏附水凝胶润滑材料的黏附性能如图10所示. 制备的黏附水凝胶润滑硅橡胶对各种基底都具有优异的黏附性,测试结果如图10(a)所示,黏附水凝胶润滑硅橡胶对316不锈钢、陶瓷和钛合金的黏附强度均可达到10 kPa以上,对于聚四氟乙烯(PTFE)的黏附强度可达到22 kPa,两种聚合物之间界面处的强电负性
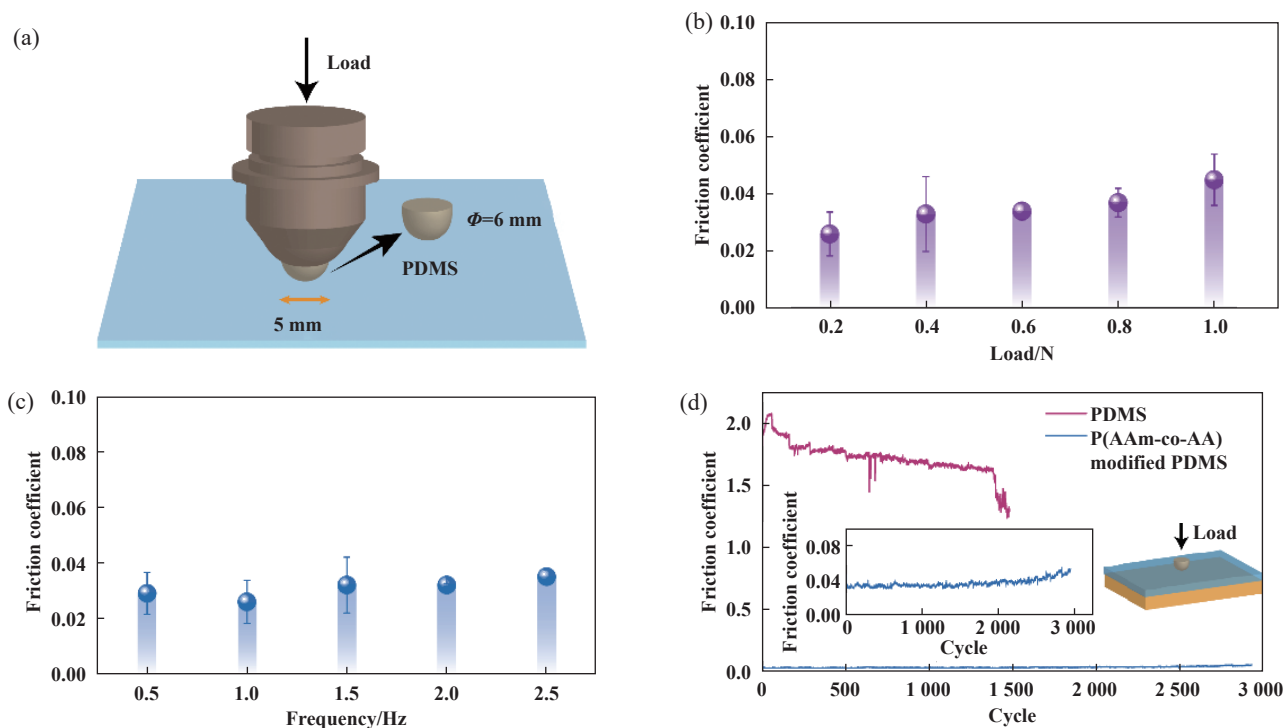


Fig. 8 Tribological properties of PDMS surface modified hydrogels: (a) friction demonstration; (b) load; (c) frequency; (d) wear resistance

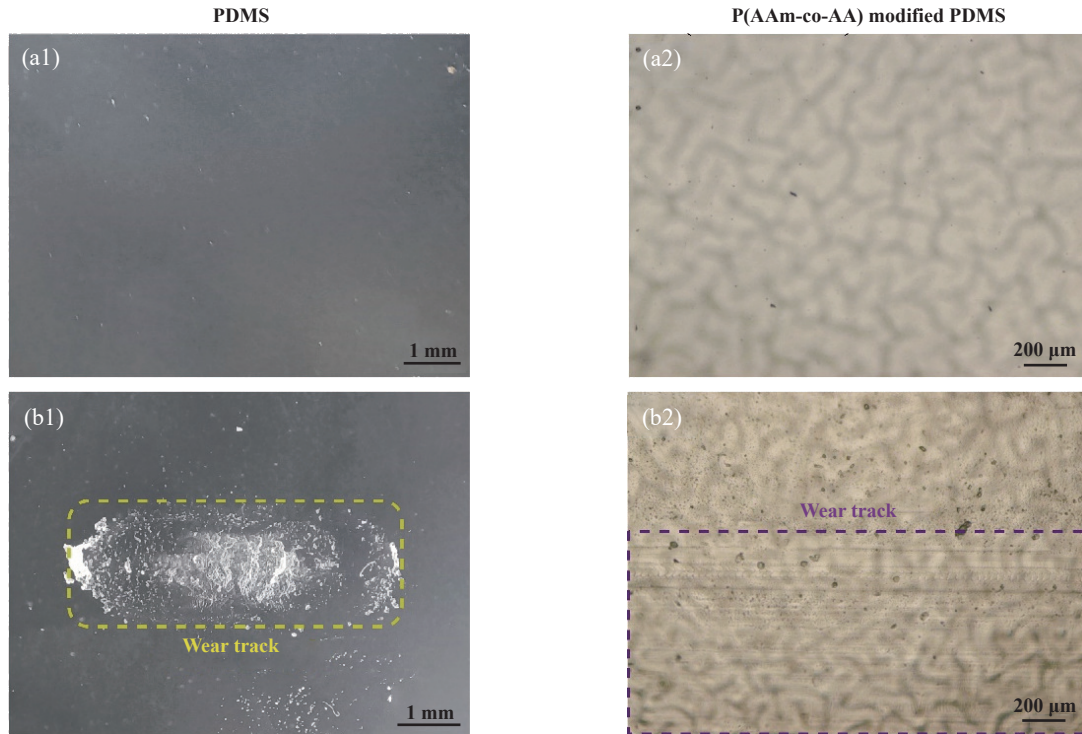图 8 PDMS表面修饰水凝胶后的摩擦学性能:(a)摩擦演示;(b)载荷;(c)频率;(d)耐磨性

Fig. 9　SEM micrographs of PDMS and adhesive hydrogel lubricated silicone rubber before and
after friction test: (a1, a2) before; (b1, b2) after
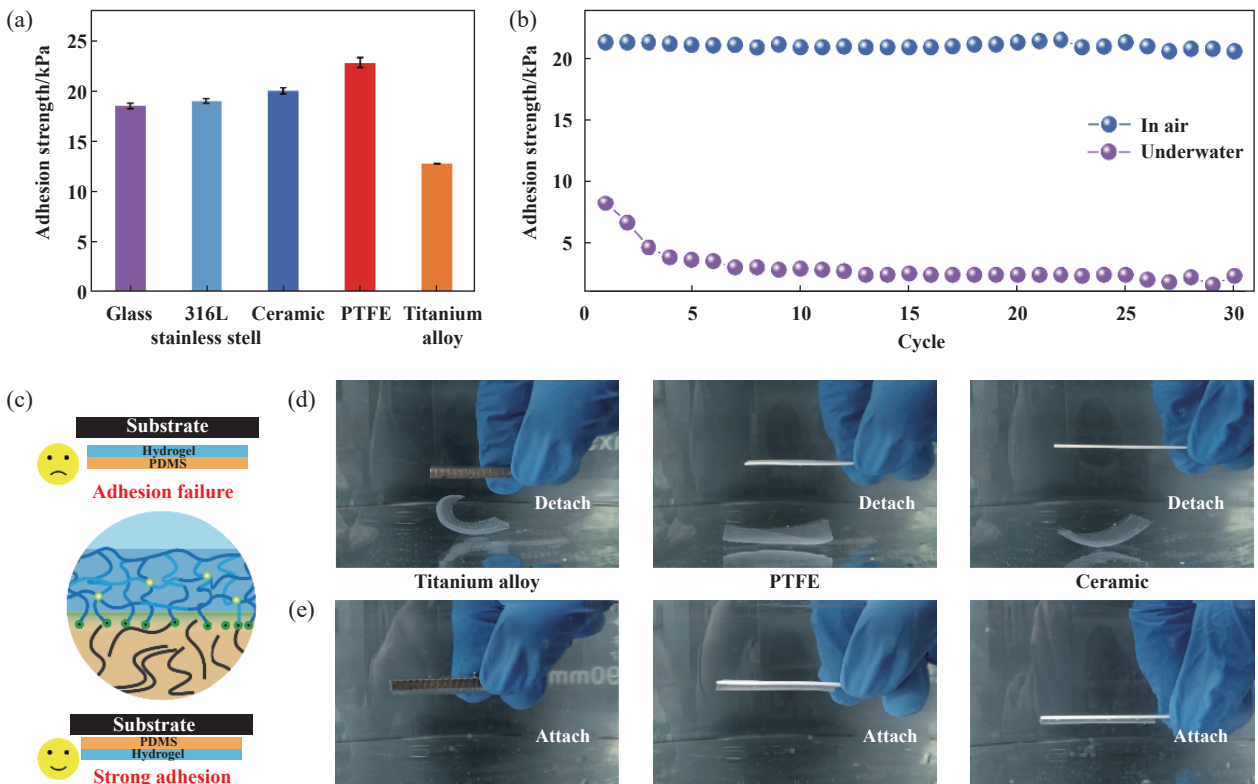
图 9　PDMS和可黏附水凝胶润滑硅橡胶摩擦测试前后表面形貌的SEM照片



Fig. 10　Adhesive properties test of adhesive hydrogel lubricating materials: (a) adhesive properties of different substrates;
(b) repeated adhesion, (c) double-sided adhesion of adhesive hydrogel lubricated silicone rubber, underwater
adhesion of titanium alloy, PTFE and ceramic: (d) hydrogel layer; (e) adhesive layer

图 10　可黏附水凝胶润滑材料的黏附性能测试: (a)不同基底的黏附性能; (b)重复黏附性能, (c)可黏附水凝胶润滑硅
橡胶双面黏附性, 钛合金、PTFE、陶瓷的水下黏附情况: (d)水凝胶层; (e)黏附层

差异,主要是基于聚四氟乙烯中的氟原子和PDMS中的氢原子之间的强电负性差异,从而诱导产生强烈的可重整的偶极—偶极子相互作用,这些作用力为这两种材料提供了额外的结合力[40]. 可重复黏附性能对于其应用至关重要,可反复使用或随时更换. 如图10(b)所示,在经历10次的黏附/脱附过程后,所制备的润滑硅橡胶仍然具有优异的黏附性能. 另外润滑硅橡胶具有两面不同的黏附性[图10(c)],PDMS黏附面对钛合金、PTFE以及陶瓷表现出良好的水下黏附性,而亲水性水凝胶层在水下对钛合金和陶瓷等不存在黏附力,直接从材料表面脱落. 底部PDMS赋予水凝胶可黏附性使其具有广泛的应用前景.

## 3 结论

a. 基于PDMS低交联度时的黏附性以及油溶性引发剂在PDMS表面的吸附,水凝胶预聚水溶液在PDMS表面原位生长聚合,得到可黏附水凝胶润滑硅橡胶.

b. 水凝胶润滑硅橡胶双面具有完全不同的结构,并且两者交界部分为一整体,结合紧密.

c. 经各参数的优化,发现丙烯酸与丙烯酰胺摩尔比为1∶1,力学性能和摩擦学性能最好,而水凝胶中交联剂含量越高,摩擦系数越低. PDMS中基底模量会影响上层水凝胶的摩擦系数,固化剂比例为30∶1时具有较好的机械性能,较低的摩擦系数以及较好的黏附性能.

d. 制备的水凝胶润滑硅橡胶具有功能不对称性,底面具有水下黏附特性,上表面赋予硅橡胶减摩抗磨性能,并且底面具有非常好的多次可重复黏附性能. 该硅橡胶将水凝胶的使用范围拓展,有望应用于生物医疗器械表面的润滑改性等领域.

## 参 考 文 献

[ 1 ] Hong S, Sycks D, Chan H F, et al. 3D printing of highly stretchable and tough hydrogels into complex, cellularized structures[J]. Advanced Materials (Deerfield Beach, Fla), 2015, 27(27): 4035–4040. doi: 10.1002/adma.201501099.

[ 2 ] Gao Yang, Jia Fei, Gao Guanghui. Transparent and conductive amino acid-tackified hydrogels as wearable strain sensors[J]. Chemical Engineering Journal, 2019, 375: 121915. doi: 10.1016/j.cej.2019.121915.

[ 3 ] Luo Jun, Yang Jiaojiao, Zheng Xiaoran, et al. A highly stretchable, real-time self-healable hydrogel adhesive matrix for tissue patches and flexible electronics[J]. Advanced Healthcare Materials, 2020, 9(4): 1901423. doi: 10.1002/adhm.201901423.

[ 4 ] Duan Xiangyu, Yu Jingyi, Zhu Yaxun, et al. Large-scale spinning approach to engineering knittable hydrogel fiber for soft robots[J]. ACS Nano, 2020, 14(11): 14929–14938. doi: 10.1021/acsnano.

0c04382.

[ 5 ] Du Xinchen, Hou Yujie, Wu Le, et al. An anti-infective hydrogel adhesive with non-swelling and robust mechanical properties for sutureless wound closure[J]. Journal of Materials Chemistry B, 2020, 8(26): 5682–5693. doi: 10.1039/d0tb00640h.

[ 6 ] Liao Meihong, Wan Pengbo, Wen Jiangru, et al. Wearable, healable, and adhesive epidermal sensors assembled from mussel-inspired conductive hybrid hydrogel framework[J]. Advanced Functional Materials, 2017, 27(48): 1703852. doi: 10.1002/adfm.201703852.

[ 7 ] Lei Dai, Zhang Liqiang, Wang Baobin, et al. Multifunctional self-assembling hydrogel from guar gum[J]. Chemical Engineering Journal, 2017, 330: 1044–1051. doi: 10.1016/j.cej.2017.08.041.

[ 8 ] Cheng Huiru, Zhang Dekun, Shen Yanqiu, et al. Friction Properties of Poly (vinyl alcohol)/Hydroxylapatite Hydrogel Prepared by Compound *in situ* with Sol-gel Method[J]. Tribology, 2008, 28(5): 422–427 (in Chinese) [程慧茹, 张德坤, 沈艳秋, 等. 沉淀法制备PVA/HA复合水凝胶的摩擦性能研究[J]. 摩擦学学报, 2008, 28(5): 422–427]. doi: 10.16078/j.tribology.2008.05.017.

[ 9 ] Rong Mingming, Ma Shuanhong, Cai Meirong, et al. Preparation of amphipathic graphene oxide/poly(acrylic acid-methyl methacrylate) composite hydrogel and the study on its tribological property under media regulation[J]. Tribology, 2018, 38(3): 309–318 (in Chinese) [荣明明, 麻拴红, 蔡美荣, 等. 两亲性氧化石墨烯/聚(丙烯酸-甲基丙烯酸甲酯)复合水凝胶的制备及介质调控的摩擦学性能研究[J]. 摩擦学学报, 2018, 38(3): 309–318]. doi: 10.16078/j.tribology.2018.03.008.

[10] Shen Yanqiu, Zhang Dekun, Ge Shirong. Contact deformation and friction performance of start-up for PVA/HA composite hydrogel[J]. Tribology, 2008, 28(2): 97–102 (in Chinese) [沈艳秋, 张德坤, 葛世荣. 聚乙烯醇/纳米羟基磷灰石复合水凝胶的接触变形与启动摩擦特性研究[J]. 摩擦学学报, 2008, 28(2): 97–102]. doi: 10.16078/j.tribology.2008.02.017.

[11] Qu Minghai, Liu Hui, Yan Changyou, et al. Layered hydrogel with controllable surface dissociation for durable lubrication[J]. Chemistry of Materials, 2020, 32(18): 7805–7813. doi: 10.1021/acs.chemmater.0c02450.

[12] Piers E M, Maria P, Jennifer L P, et al. A low friction, biphasic and boundary lubricating hydrogel for cartilage replacement[J]. Acta Biomaterialia, 2018, 65: 102–111. doi: 10.1016/j.actbio.2017.11.002.

[13] Wang Jian, Zhang Xuewei, Zhang Shuang, et al. Semi-convertible hydrogel enabled photoresponsive lubrication[J]. Matter, 2021, 4(2): 675–687. doi: 10.1016/j.matt.2020.11.018.

[14] Rao Ping, Sun Taolin, Chen Liang, et al. Tough hydrogels with fast, strong, and reversible underwater adhesion based on a multiscale design[J]. Advanced Materials (Deerfield Beach, Fla), 2018, 30(32): e1801884. doi: 10.1002/adma.201801884.

[15] Lee B P, Messersmith P B, Israelachvili J N, et al. Mussel-inspired adhesives and coatings[J]. Annual Review of Materials Research,

2011, 41: 99–132. doi: 10.1146/annurev-matsci-062910-100429.

[16] Han Lu, Wang Menghao, Prieto-López L O, et al. Self-hydrophobization in a dynamic hydrogel for creating nonspecific repeatable underwater adhesion[J]. Advanced Functional Materials, 2019, 30(7): 1907064. doi: 10.1002/adfm.201907064.

[17] Han Lu, Lu Xiong, Liu Kezhi, et al. Mussel-inspired adhesive and tough hydrogel based on nanoclay confined dopamine polymerization[J]. ACS Nano, 2017, 11(3): 2561–2574. doi: 10.1021/acsnano.6b05318.

[18] Han Lu, Lu Xiong, Wang Menghao, et al. A mussel-inspired conductive, self-adhesive, and self-healable tough hydrogel as cell stimulators and implantable bioelectronics[J]. Small, 2017, 13(2): 1601916. doi: 10.1002/smll.201601916.

[19] Yu Yan, Yuk H, Parada G A, et al. Multifunctional "hydrogel skins" on diverse polymers with arbitrary shapes[J]. Advanced Materials, 2019, 31(7): 1807101. doi: 10.1002/adma.201807101.

[20] Xu Rongnian, Zhang Yunlei, Ma Shuanhong, et al. A universal strategy for growing a tenacious hydrogel coating from a sticky initiation layer[J]. Advanced Materials, 2022, 34(11): 2108889. doi: 10.1002/adma.202108889.

[21] Cui Chunyan, Wu Tengling, Chen Xinyu, et al. A Janus hydrogel wet adhesive for internal tissue repair and anti-postoperative adhesion[J]. Advanced Functional Materials, 2020, 30(49): 2005689. doi: 10.1002/adfm.202005689.

[22] Feng Haiyan, Zhang Jianbin, Yang Wufang, et al. Transparent Janus hydrogel wet adhesive for underwater self-cleaning[J]. ACS Applied Materials & Interfaces, 2021, 13(42): 50505–50515. doi: 10.1021/acsami.1c12696.

[23] Li Wei, Li Xiaofeng, Zhang Xintao, et al. Flexible Poly(vinyl alcohol)-Polyaniline Hydrogel Film with Vertically Aligned Channels for an Integrated and Self-Healable Supercapacitor[J]. ACS Applied Energy Materials, 2020, 3(9): 9408–9416. doi: 10.1021/acsaem.0c01794.

[24] Wang Zhenxing, Wu Xiaochun, Dong Jiamei, et al. Porifera-inspired cost-effective and scalable "porous hydrogel sponge" for durable and highly efficient solar-driven desalination[J]. Chemical Engineering Journal, 2022, 427: 130905. doi: 10.1016/j.cej.2021.130905.

[25] Jin Xuting, Song Li, Yang Hongsheng, et al. Stretchable supercapacitor at −30 °C[J]. Energy & Environmental Science, 2021, 14(5): 3075–3085. doi: 10.1039/D0EE04066E.

[26] Wan Xizi, Gu Zhen, Zhang Feilong, et al. Asymmetric Janus adhesive tape prepared by interfacial hydrosilylation for wet/dry amphibious adhesion[J]. NPG Asia Materials, 2019, 11: 49. doi: 10.1038/s41427-019-0150-x.

[27] Lin Shaoting, Yang Yueying, Ni Jiahua, et al. Stretchable anti-fogging tapes for diverse transparent materials[J]. Advanced Functional Materials, 2021, 31(36): 2103551. doi: 10.1002/adfm.202103551.

[28] Yuk H, Zhang Teng, Parada G A, et al. Skin-inspired hydrogel-elastomer hybrids with robust interfaces and functional microstructures[J]. Nature Communications, 2016, 7: 12028. doi: 10.1038/ncomms12028.

[29] Zheng S Y, Yu H C, Yang C, et al. Fracture of tough and stiff metallosupramolecular hydrogels[J]. Materials Today Physics, 2020, 13: 100202. doi: 10.1016/j.mtphys.2020.100202.

[30] Dai Lixin, Zhang Wei, Sun Lu, et al. Highly stretchable and compressible self-healing P(AA-co-AAm)/CoCl2 hydrogel electrolyte for flexible supercapacitors[J]. ChemElectroChem, 2019, 6(2): 467–472. doi: 10.1002/celc.201801281.

[31] Deng Lin, Wang Chunhao, Li Zichen, et al. Re-examination of the "zipper effect" in hydrogen-bonding complexes[J]. Macromolecules, 2010, 43(6): 3004–3010. doi: 10.1021/ma902601d.

[32] Li Ting xi, Kong Na, Wu Sha sha, et al. Synthesis and performance of super absorbent resin with acrylic acid-acrylamide[J]. Materials Science Forum, 2011, 687: 523–527. doi: 10.4028/www.scientific.net/msf.687.523.

[33] Wen Hai bo, Gao Xin, Zhang Heng, et al. Water absorbency study of the low-cost composite: Eupatorium adenophorum-graft-acrylic acid/acrylamide[J]. Advanced Materials Research, 2013, 634–638: 2098–2105. doi: 10.4028/www.scientific.net/amr.634-638.2098.

[34] Wang Zhongnan, Li Jinjin, Liu Yuhong, et al. Macroscale superlubricity achieved between zwitterionic copolymer hydrogel and sapphire in water[J]. Materials & Design, 2020, 188: 108441. doi: 10.1016/j.matdes.2019.108441.

[35] Lai Shuili, Han Wujun, Yuan Dan. Synthesis of P(AA-AM)/attapulgite clay SAR under microwave irradiation[J]. Journal of Macromolecular Science, Part A, 2010, 48(1): 31–36. doi: 10.1080/10601325.2011.528304.

[36] Zhan Xiaoyuan, Wang Fang, Li Xingwei, et al. Synthesis of montmorillonite/acrylic acid/acrylamide tricopolymer and its super absorbent properties[J]. Polymers and Polymer Composites, 2014, 22(5): 489–494. doi: 10.1177/096739111402200510.

[37] Gao Luyao, Zhao Xiaoduo, Ma Shuanhong, et al. Constructing a biomimetic robust bi-layered hydrophilic lubrication coating on surface of silicone elastomer[J]. Friction, 2022, 10(7): 1046–1060. doi: 10.1007/s40544-021-0513-5.

[38] Rong Mingming, Liu Hui, Scaraggi M, et al. High lubricity meets load capacity: cartilage mimicking bilayer structure by brushing up stiff hydrogels from subsurface[J]. Advanced Functional Materials, 2020, 30(39): 2004062. doi: 10.1002/adfm.202004062.

[39] Zhang Youchen, Bao Lei. Tribological properties of PAMPS-PAAM interpenetrating polymer network hydrogel[J]. Tribology, 2012, 32(4): 396–401 (in Chinese) [张有忱, 鲍磊. PAMPS-PAAM互穿网络凝胶的摩擦性能研究[J]. 摩擦学学报, 2012, 32(4): 396–401]. doi: 10.16078/j.tribology.2012.04.010.

[40] Sealy C. Universal adhesive works under water[J]. Materials Today, 2018, 21(10): 1001. doi: 10.1016/j.mattod.2018.10.020.